Neuron, Vol. 47, 85–100, July 7, 2005, Copyright ©2005 by Elsevier Inc. DOI 10.1016/j.neuron.2005.05.013

# The Rho-Specific GEF Lfc Interacts with Neurabin and Spinophilin to Regulate Dendritic Spine Morphology

**Xiaozhou P. Ryan,[1] Jacqueline Alldritt,[2] Per Svenningsson,[1] Patrick B. Allen,[3] Gang-Yi Wu,[2,*] Angus C. Nairn,[1,3,*] and Paul Greengard[1]**

[1]Laboratory of Molecular and Cellular Neuroscience
Rockefeller University
1230 York Avenue
New York, New York 10021

[2]Department of Molecular Physiology and Biophysics
Baylor College of Medicine
Houston, Texas 77030

[3]Department of Psychiatry
Yale University School of Medicine
New Haven, Connecticut 06508

## Summary

**Neurabin and spinophilin are homologous protein phosphatase 1 and actin binding proteins that regulate dendritic spine function. A yeast two-hybrid analysis using the coiled-coil domain of neurabin revealed an interaction with Lfc, a Rho GEF. Lfc was highly expressed in brain, where it interacted with either neurabin or spinophilin. In neurons, Lfc was largely found in the shaft of dendrites in association with microtubules but translocated to spines upon neuronal stimulation. Moreover, expression of Lfc resulted in reduction in spine length and size. Both the translocation and the effect on spine morphology depended on the coiled-coil domain of Lfc. Coexpression of neurabin or spinophilin with Lfc resulted in their clustering together with F-actin, a process that depended on Rho activity. Thus, interaction between Lfc and neurabin/spinophilin selectively regulates Rho-dependent organization of F-actin in spines and is a link between the microtubule and F-actin cytoskeletons in dendrites.**

## Introduction

Dendritic spines are specialized protrusions from neuronal dendrites that receive the majority of excitatory input in the central nervous system. Recent studies have found that spines are highly dynamic, changing size and shape during development as well as in the adult brain (Bonhoeffer and Yuste, 2002; Halpain, 2000; Matus, 2000; Segal and Andersen, 2000; Yuste and Bonhoeffer, 2004). These dynamic properties are thought to be fundamental to the function of dendritic spines and to contribute to the efficacy and plasticity of synaptic transmission. The principle cytoskeletal component of dendritic spines is F-actin, and the ability of spines to change shape has been attributed to the rapid regulation of the assembly and disassembly of the actin cytoskeleton. However, despite growing evidence for roles of a variety of actin binding proteins in spines, the molecular mechanisms that control spine morphology are still not well understood.

Neurabin and the structurally related protein, spinophilin, are protein phosphatase 1 (PP1) and actin binding proteins that are involved in regulation of dendritic spine function and morphology (Allen et al., 1997; MacMillan et al., 1999; Nakanishi et al., 1997). Spinophilin, named for its enrichment in dendritic spines, and neurabin, named for its actin binding properties in neurons, are localized to spines via a conserved N-terminal F-actin binding domain (Grossman et al., 2002). Neurabin and spinophilin share a PP1 binding domain that serves to localize PP1 to dendritic spines (Allen et al., 1997; Hsieh-Wilson et al., 1999; Ouimet et al., 1995), where it is able to regulate synaptic signal transduction through its ability to dephosphorylate substrates that include the GluR1 and NR1 subunits of AMPA and NMDA glutamate receptors, $Ca^{2+}$ channels, and autophosphorylated CaM kinase II (Lisman and Zhabotinsky, 2001; Wang et al., 1994; Westphal et al., 1999; Yan et al., 1999). Indeed, studies of spinophilin-deficient mice have provided support for a role of PP1 targeting in the regulation of AMPA and NMDA receptor function, as well as in the regulation of long-term depression (Feng et al., 2000).

Spinophilin and neurabin are likely to influence dendritic spine morphology through their interaction with F-actin. Both proteins bind to the sides of F-actin filaments, and at least in vitro, both proteins can cross-link or bundle actin filaments (Hsieh-Wilson et al., 2003; Nakanishi et al., 1997; Satoh et al., 1998; Stephens and Banting, 2000). Moreover, spinophilin-deficient mice exhibit a marked increase in spine density during development, and neurons from knockout mice exhibit a large increase in filopodial protrusions when cultured at low density (Feng et al., 2000). Thus, spinophilin, and possibly neurabin, may either facilitate spine retraction during maturation or suppress the initial outgrowth of spines from the dendrite.

In addition to the F-actin and PP1 binding domains, both neurabin and spinophilin contain a central PSD95/DLG/ZO-1 (PDZ) domain and a C-terminal coiled-coil domain. The PDZ domain may interact with kalirin-7, a rac-specific GDP-GTP exchange factor (Penzes et al., 2001), and p70 S6 kinase (Buchsbaum et al., 2003; Burnett et al., 1998). Neurabin and spinophilin have been shown to interact via their coiled-coil domains (MacMillan et al., 1999; Oliver et al., 2002; Terry-Lorenzo et al., 2002). In preliminary studies, we found that the coiled-coil domains of either neurabin or spinophilin appeared to influence their subcellular localization. To identify binding partners, we carried out a yeast two-hybrid analysis using the coiled-coil domain of neurabin. This revealed an interaction between neurabin and Lfc (*L*bc [lymphoid blast crisis]'s *f*irst *c*ousin), a Rho guanine nucleotide exchange factor (GEF). Lfc was originally identified in a truncated form as a mouse oncogene. Our studies show that native Lfc is highly expressed in neurons in the central nervous system, especially in forebrain regions including cortex and hippocampus. While

*Correspondence: gangyiw@bcm.tmc.edu (G.-Y.W.); angus.nairn@yale.edu (A.C.N.)

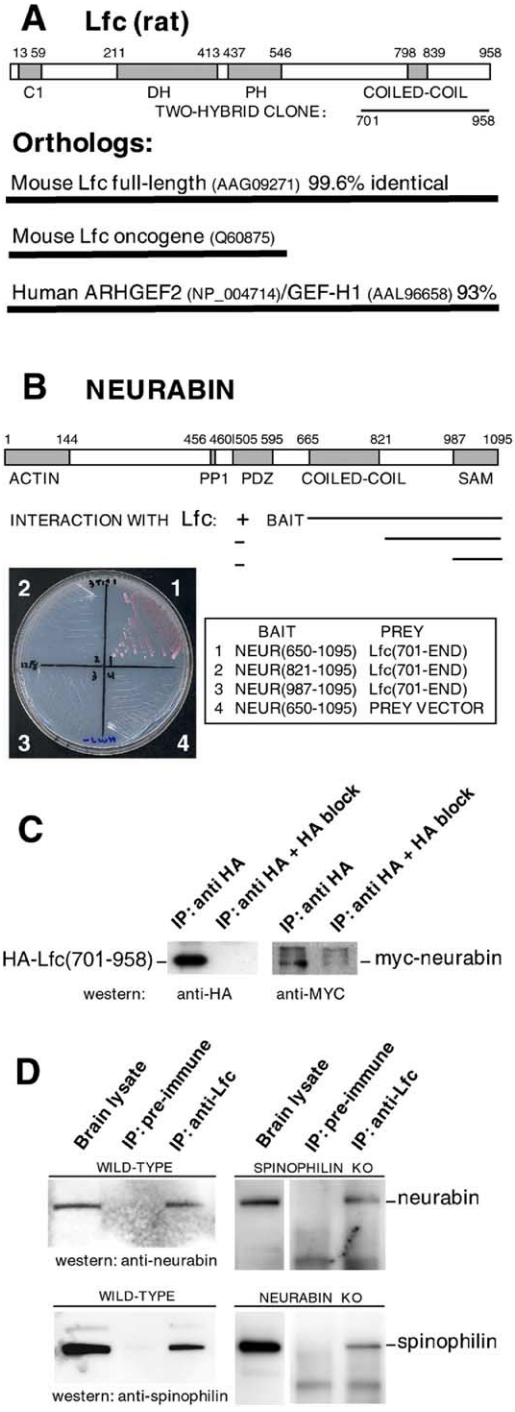


Figure 1. Lfc, a Rho GEF, Interacts with Neurabin and Spinophilin in Neurons

(A) The domain organization of full-length rat Lfc is compared to its mouse and human orthologs. Based on the position of different Met residues, three alternative N-terminal sequences were predicted for rat Lfc (the Met within the sequence TREKEKMKEAKD was defined as residue 1).

(B) The region of neurabin used as bait in the two-hybrid screen is shown and compared to other fragments of neurabin used to confirm the interaction of the coiled-coil region with Lfc. The left panel shows the growth capability on selective medium of yeast cells expressing different neurabin-based baits with Lfc(701–958) (quadrants 1–3) or with a control vector (quadrant 4).

(C) HA-Lfc(701–958) and Myc-neurabin were coexpressed in N2a cells, and immunoprecipitation was performed using an anti-HA antibody in the absence or presence of an HA antigen peptide. Samples were analyzed by SDS-PAGE, and immunoblotting was carried out with either anti-HA (left panels) or anti-Myc (right panels) antibodies.

(D) Homogenates were prepared from wild-type (left panels), spinophilin knockout, or neurabin knockout mice (right panels), and immunoprecipitation was performed using anti-Lfc antibody or control preimmune serum. Samples were analyzed by SDS-PAGE, and immunoblotting was carried out with either anti-neurabin (upper panels) or anti-spinophilin (lower panels) antibodies. An aliquot of each brain lysate (20 μg) was also separated by SDS-PAGE and analyzed by immunoblotting.

the Rho family of small GTPases has been implicated in various aspects of neuronal function, these studies have largely focused on Rac, and little is known about the regulation of Rho in dendrites and spines. Our biochemical and morphological studies indicate that recruitment of Lfc by neurabin/spinophilin selectively regulates Rho-dependent organization of F-actin in spines leading to altered spine morphology. Moreover, our studies show that under basal conditions Lfc is associated with microtubules in dendrites, but that following neuronal stimulation Lfc translocates to spines. The interaction of Lfc with neurabin and spinophilin may therefore represent a link between the microtubule cytoskeleton in dendrites and the F-actin cytoskeleton in spines.

## Results

### The Rho Family GEF Lfc Interacts with Neurabin and Spinophilin

A series of fusion proteins, all of which contain the F-actin binding domain of neurabin coupled to enhanced green fluorescent protein (GFP), were expressed in the neuroblastoma cell line N2a, and their subcellular distribution(s) was compared with the F-actin (see Figure S1 in the Supplemental Data available with this article online). While neurabin(1–485) and neurabin(1–652) colocalized with F-actin throughout the cell, the localizations of neurabin(1–821) and full-length neurabin were restricted to the base of filopodia and cortical actin. Studies with full-length spinophilin gave similar results (see also Stephens and Banting, 2000). These results raised the possibility that protein interactions mediated by the coiled-coil domain might influence neurabin function.

Using neurabin(650–1095) as a yeast two-hybrid bait, and a GAL4-based rat cDNA expression library, a screen of $2 \times 10^5$ yeast transformants identified several clones that passed the appropriate controls for interaction specificity. One prey cDNA class encoded spinophilin and was represented by six clones starting at various positions between residues 644 and 712, extending to the C terminus, a region that contains the coiled-coil domain of spinophilin. This finding is in agreement with previous reports that spinophilin and neurabin can exist in the same complex (Oliver et al., 2002; Terry-Lorenzo et al., 2002). A second interacting class (two clones) encoded a polypeptide that is also predicted to pos-

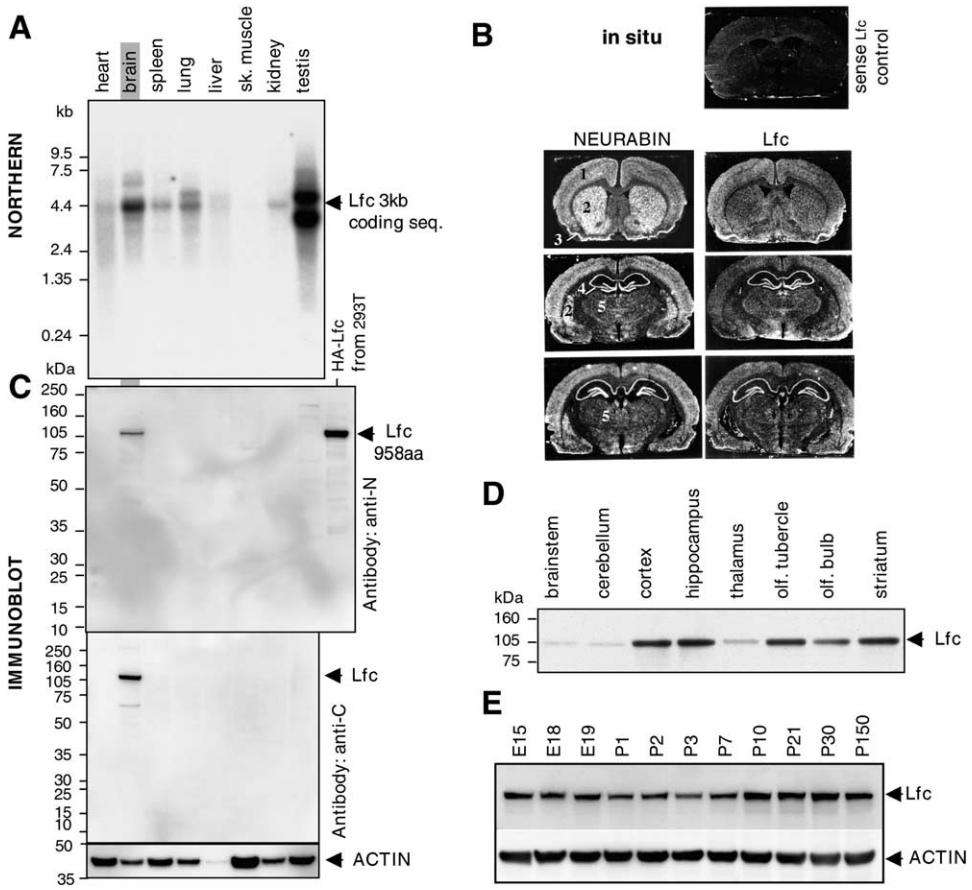


Figure 2. Full-Length Lfc Is Highly Expressed in Brain

(A) Northern blot detection of Lfc mRNA in rat tissues.

(B) Comparison of the levels of neurabin and Lfc gene expression by in situ hybridization using $^{35}$S-labeled complementary riboprobes. The upper panel shows a control using a sense Lfc probe. (B1) Cortex; (B2) striatum; (B3) piriform cortex; (B4) hippocampus; (B5) thalamus.

(C) Immunoblot analysis of Lfc in rat tissues using a polyclonal antibody raised against Lfc(1–588) (anti-N) or Lfc(701–958) (anti-C). HA-Lfc full-length protein expressed in HEK293 cells was included as positive control. Tissue (30 μg) was analyzed; the level of total actin was analyzed as a loading control (lower panel). In spite of the widespread mRNA expression, there was no evidence for significant Lfc protein expression in any other tissue examined, even after much longer exposure of the immunoblots (data not shown).

(D) Immunoblot analysis of Lfc in brain regions (20 μg per lane) using the anti-C antibody.

(E) Developmental profile of Lfc present in mouse cortical homogenates at the embryonic (E) and postnatal (P) days indicated (anti-C antibody for Lfc; 30 μg per lane); the level of total actin was analyzed as a loading control (lower panel).

sess coiled-coil structure. The fragment identified was similar to a part of the C terminus of full-length mouse Lfc (human GEF-H1/ARHGEF2), a Rho family GEF (Glaven et al., 1996; Ren et al., 1999). Notably, the oncogenic form of Lfc (Whitehead et al., 1995) lacks the C-terminal region that includes the coiled-coil domain (Figure 1A). The complete sequence of the full-length rat Lfc cDNA was obtained using 5′ RACE. As expected, a C1 domain was found at the N terminus (in protein kinase C, this domain mediates membrane association and kinase activation via diacylglycerol binding [Nishizuka, 1992]). Dbl homology (DH) and pleckstrin homology (PH) domains followed; the DH domain accelerates guanine nucleotide exchange for Rho/Rac/Cdc42-like GTPases, and the PH domain is thought to function as a targeting or regulatory module (Blomberg et al., 1999).

Deletion mutagenesis experiments confirmed that the coiled-coil domain of neurabin was required for the two-hybrid interaction; constructs lacking the coiled-coil region [neurabin(821–1095) and (987–1095)] did not allow yeast clones to grow on selective medium (Figure 1B). Hemagglutinin (HA)-tagged Lfc(701–958) was coexpressed with Myc-neurabin in N2a cells, and an anti-HA antibody coprecipitated Myc-neurabin (Figure 1C). Coimmunoprecipitation studies using a polyclonal antibody raised against residues 701–958 of Lfc indicated that neurabin and Lfc interacted in a rat brain homogenate (Figure 1D, upper panel). Lfc also coprecipitated spinophilin from a rat brain homogenate (Figure 1D, lower panel). Since the coiled-coil region of neurabin can interact with spinophilin, a neurabin-spinophilin dimer could, in principle, interact with Lfc to form a coiled-coil trimer. Coimmunoprecipitation experiments were therefore repeated using brain homogenate from knockout mice that lack either spinophilin or neurabin. Coimmunoprecipitation of Lfc and neurabin (in the absence of spinophilin) or of Lfc and spinophilin (in the absence of neurabin) was observed, confirming the

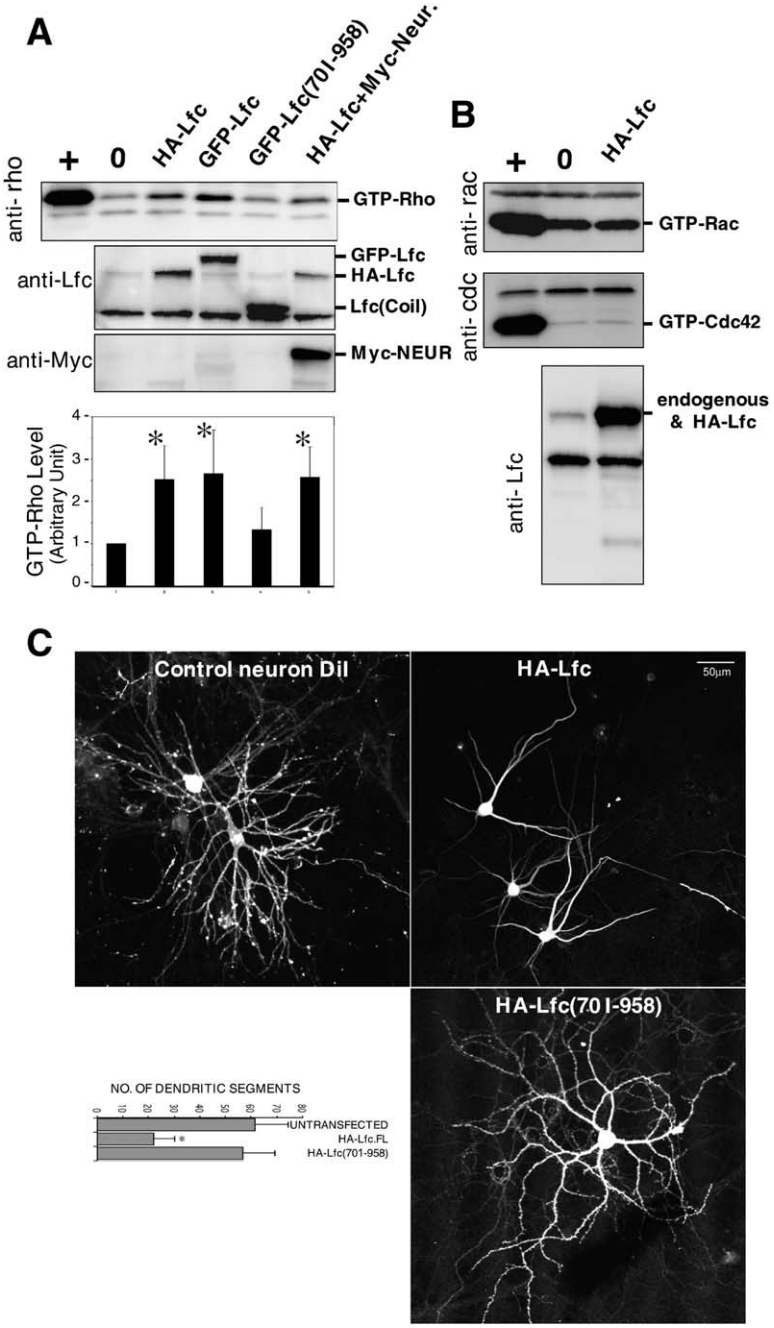


Figure 3. Lfc Is a Rho-Specific GEF that Regulates Dendritic Structure in Neurons

(A) HA-Lfc, GFP-Lfc, GFP-Lfc(701–958), or Myc-neurabin was expressed in N2a cells. 0 indicates nontransfected cells. GTP-Rho was precipitated from cell lysates using beads coated with Rhotekin, and the amount of GTP-Rho was detected by immunoblotting. As a positive control (+), lysate from untransfected cells was incubated with GTP-γS (100 μM) prior to effector binding. Immunoblotting with anti-Lfc (anti-C for all) and anti-Myc antibodies was used to confirm expression of Lfc and neurabin (lower panels). The bar graph shows normalized data for levels of GTP-Rho obtained from three separate experiments (mean ± SD; *$p < 0.05$, Student's t test). The bars are aligned with the corresponding lanes above.

(B) Assays were performed as described in (A) except that GTP-Rac or GTP-Cdc42 was precipitated using their common effector protein PAK1. GTP-Rac, GTP-Cdc42, or Lfc was detected by immunoblotting using specific antibodies. In lysates from control cells in (A) and (B), low levels of endogenous Lfc can be detected in the immunoblots.

(C) HA-Lfc (full-length) or HA-Lfc(701–958) was expressed in hippocampal neurons at 6DIV, and cells were fixed at 22DIV. HA-Lfc was detected with anti-HA antibody (right panels). The morphology of control, untransfected neurons was examined using DiI as a volume marker (left, upper panel). The scale bar (50 μm) shown in the right upper panel is appropriate for all three panels. The number of dendritic segments per neuron was measured in control and transfected neurons (bar graph, mean ± SD; *$p < 0.05$). The following numbers of neurons were counted for the bar graph in Figure 3C: untransfected (DiI stained), n = 20; HA-Lfc.FL, n = 26; HA-Lfc(701–958), n = 9 (from more than five experiments). Statistical analysis was determined using the Student's t test.

ability of Lfc to interact independently with either neurabin or spinophilin (Figure 1D).

### Full-Length Lfc Is Highly Expressed in Brain

Although the functions of oncogenic and truncated forms of Lfc have been examined in cell lines in culture, the distribution of the full-length protein has not been characterized. The tissue distribution of Lfc mRNA was investigated by Northern blotting using a probe encoding amino acids 701–958. A major mRNA of 4.4 kb was observed in brain and testis, with lower levels in other tissues (Figure 2A). The distribution of Lfc mRNA in rat brain was also examined by in situ hybridization using antisense RNA transcribed from the region of Lfc encoding amino acids 23–795. The signal was particularly high in the hippocampus and piriform cortex. In general, the expression pattern of Lfc mRNA largely overlapped with that of neurabin (Figure 2B) and spinophilin (data not shown).

The distribution of Lfc protein was investigated by immunoblotting using polyclonal antibodies raised against either amino acids 1–570 (anti-N) or 701–958 (anti-C) (Figure 2C). A single band corresponding to the expected size of full-length rat Lfc (107 kDa) was found in the brain using both antibodies. Within the brain, Lfc protein expression was high in the hippocampus, cor-

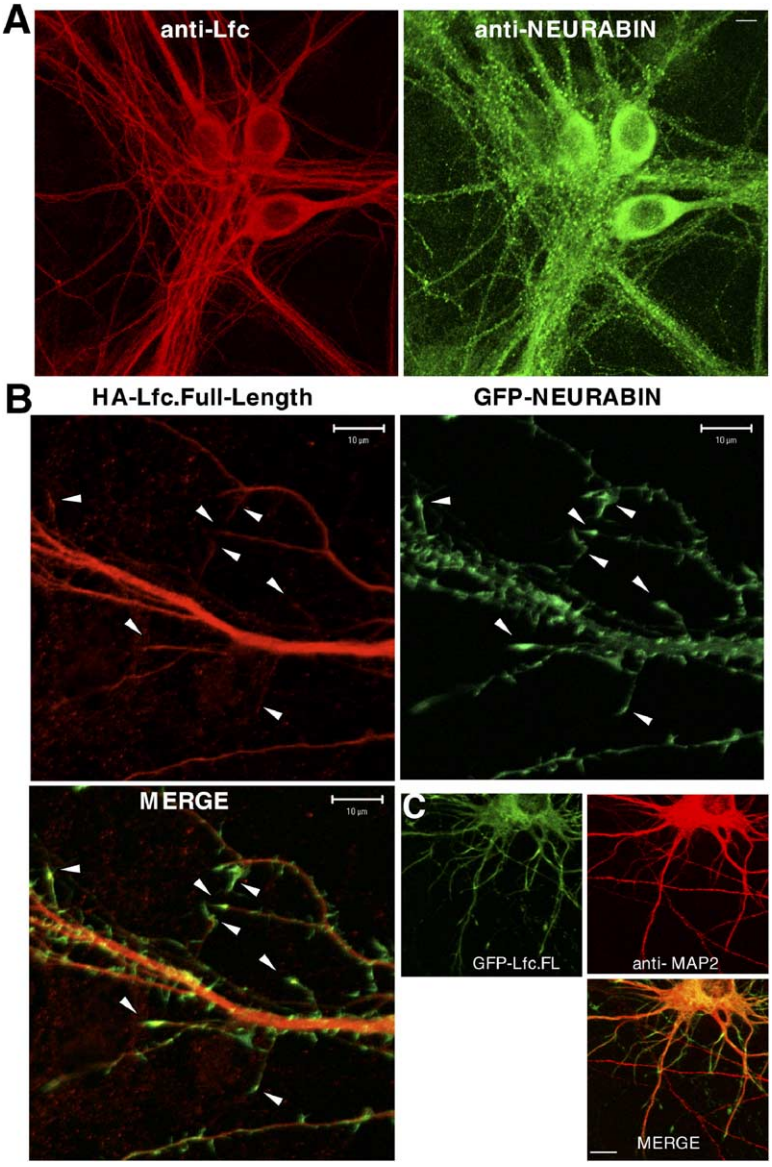


Figure 4. Localization of Lfc in Neurons

(A) Confocal photomicrograph of cultured hippocampal neurons (22DIV) immunolabeled for endogenous Lfc (red) or neurabin (green).

(B) HA-Lfc (red) and GFP-neurabin (green) were coexpressed in neurons at 8DIV, and their distribution was examined at 12DIV (the lower left panel shows a merge of the red anti-HA and green GFP signals). Arrowheads show sites of colocalization of Lfc and neurabin in small branches.

(C) GFP-Lfc (green) was expressed in hippocampal neurons (at 6DIV), and its localization at 10DIV was compared to endogenous MAP-2 detected using a specific antibody (red). The lower right panel shows a merge of the red and green signals. Scale bars, 10 μm.

tex, striatum, olfactory tubercle, and olfactory bulb, but low in the thalamus, cerebellum, and brainstem (Figure 2D). This pattern is qualitatively similar to the relative expression patterns of spinophilin and neurabin in these brain regions (Allen et al., 1999) (C.C. Ouimet, P.B.A., and P.G., unpublished data). During development, the level of Lfc was high in brain at all stages from embryonic day 15 to adult (Figure 2E).

### Lfc Stimulates GDP/GTP Exchange for RhoA, and Expression of Lfc in Neurons Prevents Dendritic Arborization

Previous studies in nonneuronal cells indicated that oncogenic Lfc and GEF-H1 function as Rho GEFs (Glaven et al., 1996; Ren et al., 1998), although it has also been suggested that oncogenic Lfc and GEF-H1 can bind to and possibly activate Rac1 (Glaven et al., 1999). To further examine the specificity of full-length Lfc, and to analyze whether neurabin might influence its interaction with GTP bound Rho/Rac/Cdc42-like GTPases, rat Lfc was expressed in N2a cells in the absence or presence of neurabin. GTP-Rho was precipitated from cell lysates using beads coated with Rhotekin, an effector protein of Rho that binds GTP-Rho, but not GDP-Rho (Ren et al., 1998). Similar assays were performed with PAK1, an effector common to both Rac and Cdc42 (Benard et al., 1999). A ~2.5-fold increase was observed in the level of GTP-Rho coprecipitated from cells expressing HA-Lfc or GFP-Lfc, as compared to mock-transfected cells, or cells expressing an Lfc fragment lacking the DH-PH domain (Figure 3A). Coexpression of Myc-neurabin did not influence the effect of Lfc on the accumulation of GTP-Rho (Figure 3A). No change in the activity of GTP-Rac or GTP-Cdc42 was detected (Figure 3B).

Rho has been implicated in various aspects of neuronal morphology and function, and many of the spe-

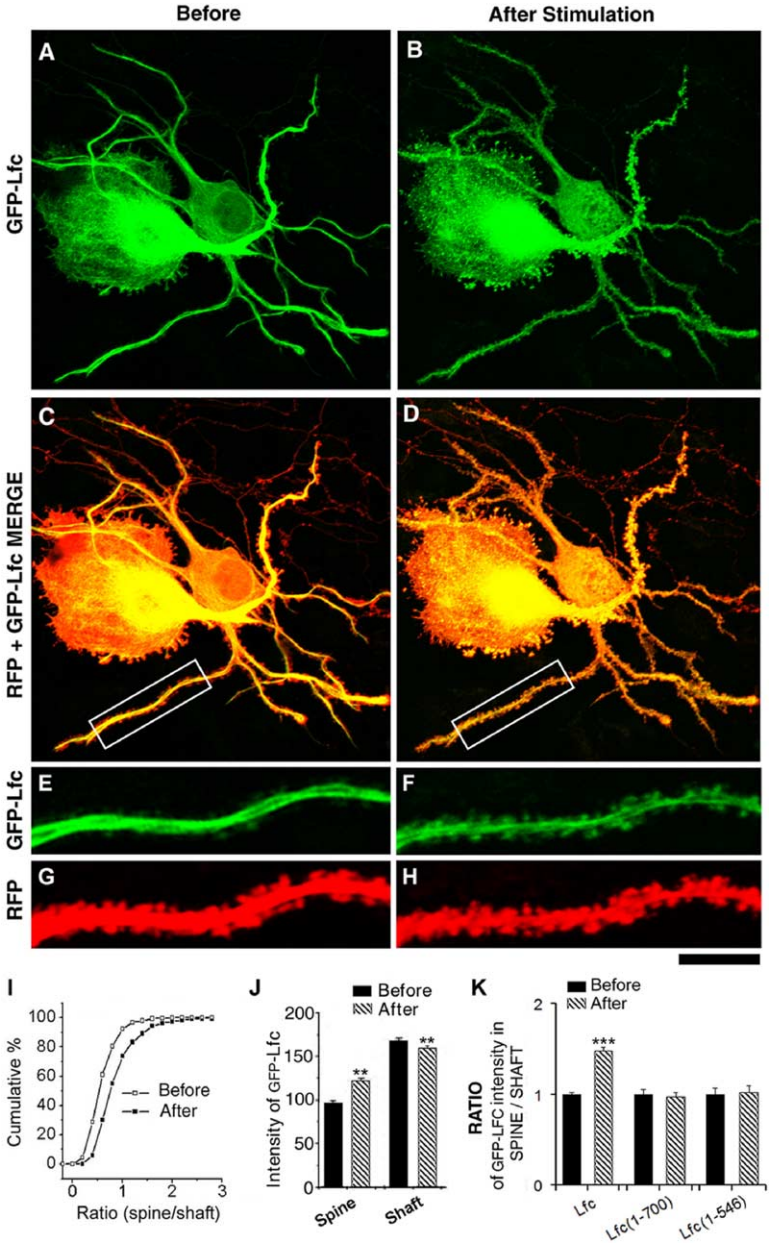


Figure 5. Redistribution of Lfc into Dendritic Spines following Depolarization

Dentate gyrus neurons were cotransfected with GFP-Lfc and RFP at 8DIV and imaged at 22DIV. (A) Under nonstimulated conditions, GFP-Lfc was mainly distributed within dendritic shafts. Note that both neurons exhibit atrophy of dendritic structure due to Lfc overexpression, and the left neuron showed a lamellipodium surrounding the soma. (B) After stimulation with 90 mM KCl in isotonic Tyrode's solution for 3 min, followed by 10 min wash with TTX Tyrode's solution, the intensity of staining of GFP-Lfc increased in many dendritic spines, and this was associated with a slight loss of GFP-Lfc signal in dendritic shafts. (C and D) are merged images of GFP-Lfc (green) and RFP (red) channels. RFP (DsRed) was used as a volume marker to monitor spine morphology before and after stimulation. Note that more spines appeared yellow after stimulation. (E–H) Higher-magnification views of the selected fields in (C) and (D) in green and red channels. There was no change in the number of dendritic spines within the observation period after the stimulation, nor was there any change in spine length, width, or area (data not shown). (I) Cumulative frequency plots of the ratio of spine to shaft intensity in control and after 90 mM KCl stimulation. There was a statistically significant difference between the two data sets (Kolmogorov-Smirnov, $p < 0.05$) (n = 417 spine-shaft pairs from five cells and three independent experiments). (J) Quantitative summary of Lfc translocation. (K) Normalized mean intensity ratio of GFP-Lfc (n = 417 spine/shaft pairs, five cells, and three independent experiments), GFP-Lfc(1–700) (n = 121 spine/shaft pairs, two cells, and two independent experiments), and GFP-Lfc(1–546) (n = 146 spine/shaft pairs, five cells, and two independent experiments) before and after stimulation. The values are means ± SEM; $^{**}p < 0.01$, $^{***}p < 0.001$ (one-way ANOVA). Scale bar, 30 μm for (A)–(D), 10 μm for (E)–(H).

cific activities of Rho are likely to be regulated by its interactions with GEF proteins including Lfc (Etienne-Manneville and Hall, 2002; Luo, 2000). To examine the possible role of Lfc in the regulation of dendritic morphology, cultured hippocampal neurons (at 6 days in vitro [DIV]) were transfected with a construct expressing full-length HA-tagged Lfc, and cells were fixed for immunocytochemistry at 22DIV. Neurons expressing full-length HA-Lfc exhibited a greatly reduced dendritic tree with fewer arborizations compared to nontransfected neurons in the same cultures, or to neurons transfected with the C terminus of Lfc [Lfc(701–958); Figure 3C]. Additional preliminary results indicate that the inhibitory effect of Lfc on dendritic arborization depends on Rho and Rho kinase activity (J.A., X.P.R., P.G., A.C.N., G.-Y.W., unpublished data). The ability of active Rho to cause retraction of dendritic branches also appears to involve regulation of the actin cytoskeleton (Nakayama et al., 2000). Whether spinophilin/neurabin might be involved in this more global effect of Rho on dendritic morphology was not examined.

### Lfc Translocates to Dendritic Spines following Neuronal Stimulation

Previous studies have suggested that the truncated oncogenic forms of Lfc and GEF-H1 interact with microtubules when overexpressed in dividing cells in culture (Glaven et al., 1996; Ren et al., 1998). Immunocytochemical analysis of endogenous Lfc in cultured hippocampal neurons showed that the protein was localized to both cell bodies and dendritic shafts (Figure 4A). Within dendrites, endogenous neurabin staining displayed a punc-

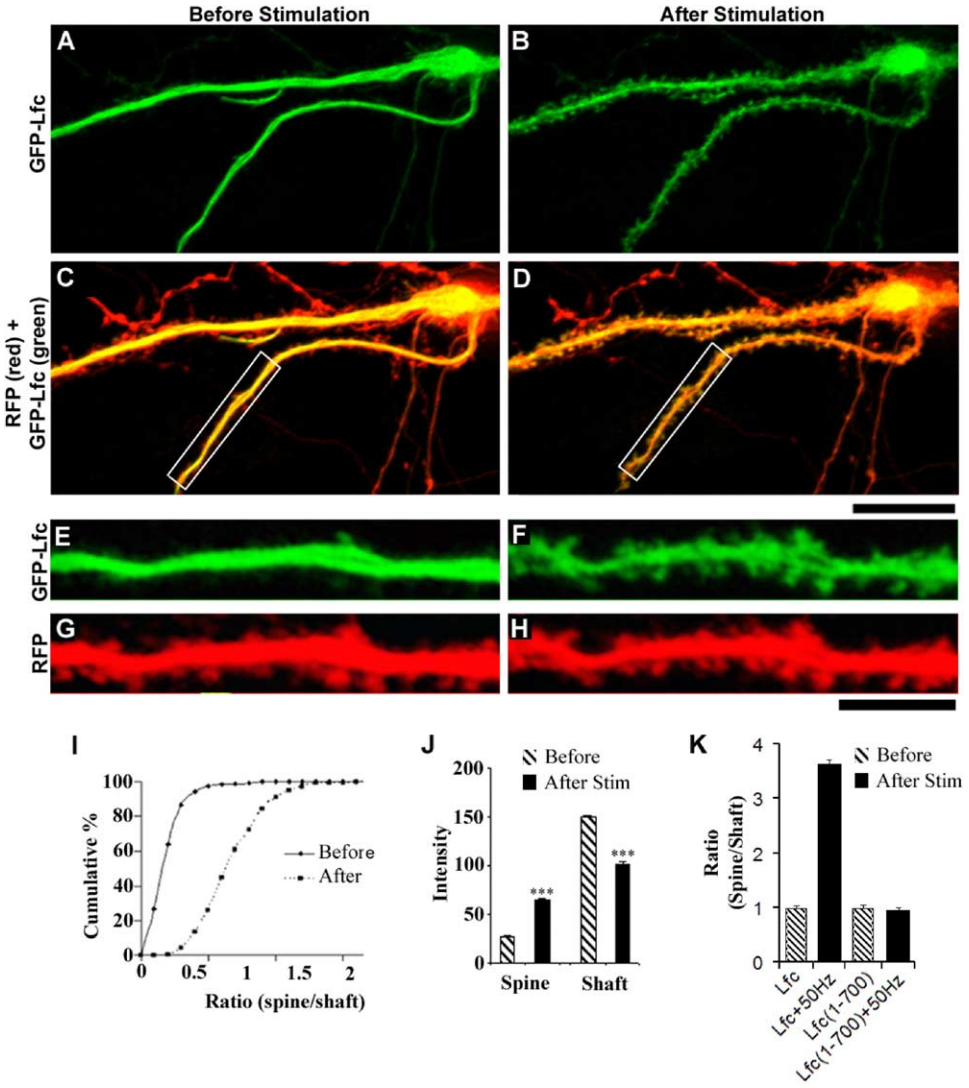


Figure 6. Redistribution of Lfc into Dendritic Spines following Field Stimulation

Dentate gyrus neurons were cotransfected with GFP-Lfc and RFP at 8DIV and imaged at 16DIV. (A) Under nonstimulated conditions, GFP-Lfc was mainly distributed within dendritic shafts. (B) After stimulation with 50 Hz field stimulation in Tyrode's solution for 20 s, the intensity of GFP-Lfc increased in many dendritic spines, and this was associated with a loss of GFP-Lfc signal in dendritic shafts. The translocation peaked around 10 min after stimulation with no obvious reversibility within 60 min (data not shown). (C) and (D) are merged images of GFP-Lfc (green) and RFP (red) channels. RFP (DsRed) was used as a volume marker to monitor spine morphology before and after stimulation. There was no change in spine length, width, area, or density following a 30 min observation period after the stimulation (see Figure S3). Note that more spines appeared yellow after stimulation. (E–H) Higher-magnification views of the selected fields in (C) and (D) in green and red channels. (I) Cumulative frequency plots of the ratio of spine to shaft intensity in control and after 50 Hz stimulation. There was a statistically significant difference between the two data sets (Kolmogorov-Smirnov, $p < 0.05$) (n = 401 spine-shaft pairs from 11 cells and two independent experiments. Similar results were found in four other experiments.) (J) Quantitative summary of Lfc translocation.

(K) Normalized mean intensity ratio of GFP-Lfc (n = 401 spine/shaft pairs, 11 cells, and two independent experiments) and GFP-Lfc(1–700) (n = 117 spine/shaft pairs, four cells, and two independent experiments) before and after stimulation. The values are means ± SEM; ***$p < 0.001$ (one-way ANOVA). Scale bar, 50 μm for (A)–(D), 20 μm for (E)–(H).

tate pattern reflecting its enrichment in dendritic spines. In transfected neurons coexpressing HA-Lfc and GFP-neurabin, HA-Lfc was largely restricted to the shaft of the dendrite, while GFP-neurabin showed enrichment in structures resembling spines or filopodia (Figure 4B). As seen from the merged images, some colocalization of HA-Lfc and GFP-neurabin was observed in the dendritic shaft and also in the tips of small branches. Further analysis of neurons expressing full-length GFP-Lfc showed a high degree of colocalization with the microtubule-associated protein MAP-2 in dendritic shafts (Figure 4C). There is some disagreement over which domain of truncated Lfc and GEF-H1 is responsible for the interaction with microtubules (Glaven et al., 1996; Krendel et al., 2002; Ren et al., 1998). Our analysis of various Lfc fragments and mutants has found that the C1 domain is necessary and sufficient for mediating the interaction with microtubules (J.A., X.P.R., P.G., A.C.N., G.-Y.W., unpublished data).

Although the microtubule and actin cytoskeletons are

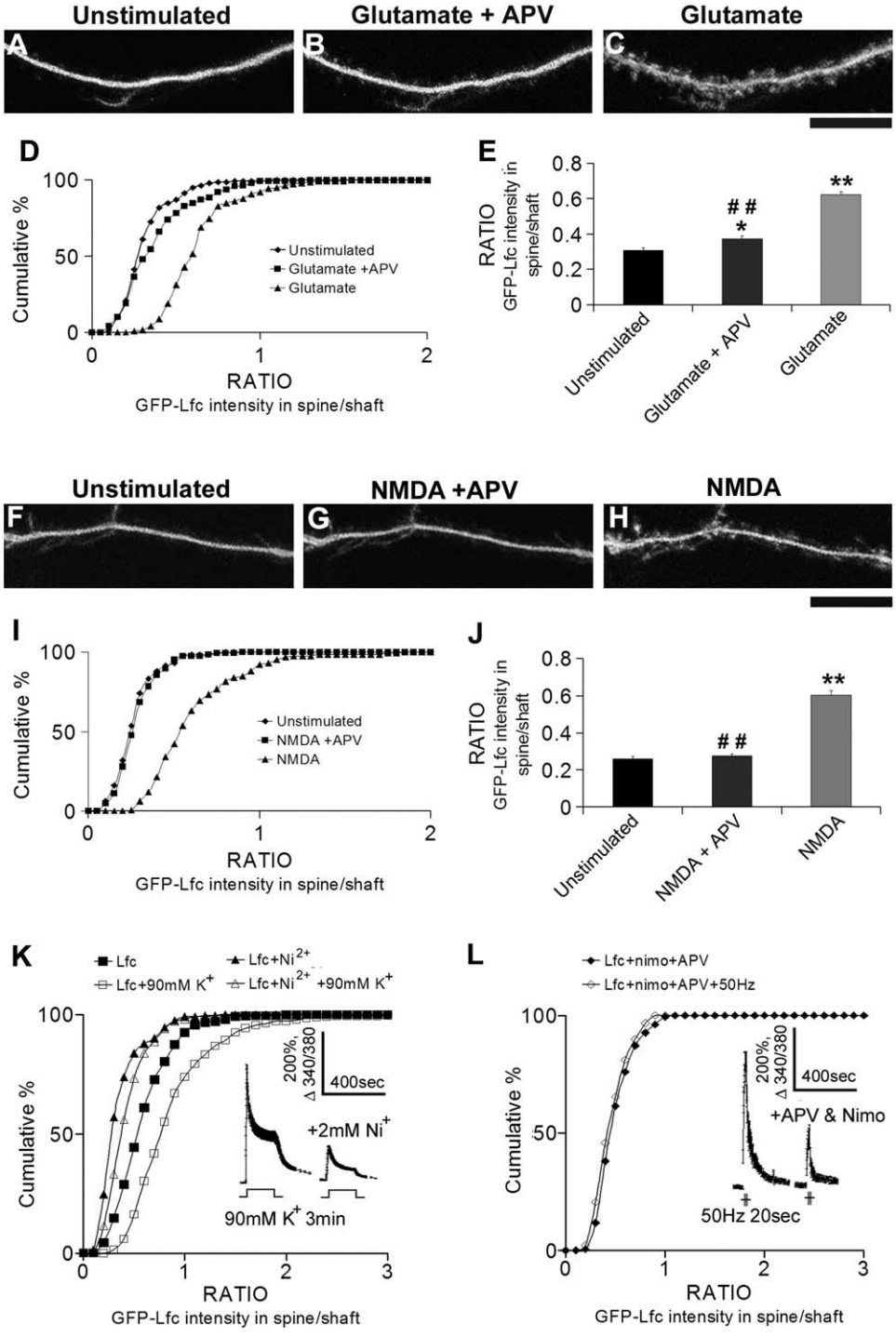


Figure 7. Glutamate Stimulates GFP-Lfc Translocation via NMDA Receptors and $Ca^{2+}$ Influx

Dentate gyrus neurons were transfected with GFP-Lfc at 8DIV and imaged at 16DIV. Neurons were stimulated with either glutamate (500 μM, 15 s) (A–E) or NMDA (10 μM, 30 min) (F–J) with or without APV (400 μM). (A)–(C) show confocal images of a dendritic segment from a single neuron before stimulation (A), after stimulation with glutamate in the presence of APV (B), and after washout of APV and restimulation with glutamate (C). (D) Cumulative frequency plot and (E) mean intensity of the ratio of spine to shaft intensity for GFP-Lfc in neurons treated with glutamate with or without APV (n = 138 spine/shaft pairs from four cells). (F)–(H) show confocal images of a dendritic segment from a single neuron before stimulation (F), after stimulation with NMDA in the presence of APV (G), and after washout of APV and restimulation with NMDA (H). (I) Cumulative frequency plot and (J) mean intensity of the ratio of spine to shaft intensity for GFP-Lfc in spines/shaft treated with NMDA with or without APV (n = 125 spine/shaft pairs from three cells). APV significantly blocked glutamate- or NMDA-induced GFP-Lfc translocation. *$p < 0.05$, **$p < 0.001$ as compared to unstimulated control; ##$p < 0.001$ compared to glutamate- or NMDA-treated neurons. Significance was determined by paired Student's t test (mean ± SEM). (K–L) Dentate gyrus neurons were transfected with GFP-Lfc at 8DIV and imaged at

apparently largely segregated to dendrites and dendritic spines, respectively, it seems likely that there will be interplay between the two cytoskeletons. Moreover, the actin cytoskeleton within spines is highly dynamic and known to be regulated by synaptic activity (Fischer et al., 1998; Fischer et al., 2000; Fukazawa et al., 2003). We therefore examined the effect of KCl-dependent depolarization and electrical stimulation on the localization of Lfc in dendrites. Dentate gyrus neurons were cotransfected with GFP-Lfc and DsRed (red fluorescent protein [RFP]) at 8DIV and imaged at 22DIV (Figure 5). Under nonstimulated conditions, GFP-Lfc was mainly distributed within dendritic shafts, with some neurons having low to moderate staining of Lfc in some of their dendritic spines (Figures 5A and 5E). After stimulation with 90 mM KCl for 3 min, followed by 10 min wash with TTX Tyrode's solution, the intensity of staining of GFP-Lfc increased in many dendritic spines, and this was associated with a loss of GFP-Lfc signal in dendritic shafts (Figures 5B and 5F; quantitation shown in Figures 5I and 5J). Treatment with 90 mM KCl did not influence the number of spines, as revealed by examination of the localization of RFP (Figures 5G and 5H). Significantly, no translocation was observed for truncated Lfc in which the coiled-coil domain was deleted [Lfc(1–700)] or in a shorter mutant protein truncated just after the PH domain [Lfc(1–546)] (Figure 5K and see Figure S2 for detailed results). Rapid translocation of Lfc from dendrites to spines was also observed in dentate gyrus neurons following field stimulation (50 Hz for 20 s) (Figure 6). The intensity of staining of GFP-Lfc increased in many dendritic spines, and this was associated with a loss of GFP-Lfc signal in dendritic shafts (Figures 6B and 6F; quantitation shown in Figures 6I and 6J). As found following $K^+$ depolarization, no translocation was observed after electrical stimulation for truncated Lfc in which the coiled-coil domain was deleted [Lfc(1–700); Figure 6K and Figure S2]. Field stimulation had no effect on spine morphology (see Figure S3).

We next examined the signaling mechanism involved in the translocation of Lfc from dendrites to spines. Direct support for the involvement of NMDA receptors was obtained from studies that showed that stimulation of neurons with either glutamate (Figures 7A–7E) or NMDA (Figures 7F–7J) resulted in rapid translocation of Lfc from dendrites to spines, effects that were blocked by the addition of APV. Moreover, the translocation was dependent on $Ca^{2+}$ influx, as addition of a high concentration of $Ni^{2+}$ (2 mM), used as a nonselective $Ca^{2+}$ blocker, largely attenuated the translocation of GFP-Lfc as well as the $Ca^{2+}$ influx (Figure 7K). In addition, no translocation was found for GFP-Lfc when $Ca^{2+}$ influx through NMDA receptors and L-type $Ca^{2+}$ channels was blocked using APV and nimodipine (Figure 7L).

### Neurabin and Lfc Association Regulates the Actin Cytoskeleton in a Rho-Dependent Manner

The functional consequence of the interaction between neurabin and Lfc was studied following their coexpression in N2a cells. In N2a cells, Myc-neurabin when expressed alone was found largely in the vicinity of the cell membrane and displayed a distribution similar to that of the cortical actin cytoskeleton (Figures 8A–8D; see also Figure S1). GFP-Lfc expressed alone was evenly distributed in the cell body and was absent from the cell nucleus. Upon coexpression, a major reorganization of both Myc-neurabin and GFP-Lfc was observed, with significant clustering of the two proteins, often at a restricted site close to the cell periphery. Similar results were obtained following coexpression of GFP-Lfc and Myc-spinophilin in N2a cells (Figure S1).

The role of this interaction, in terms of the organization of the actin and microtubule cytoskeletons, was investigated. In these studies, we used neurabin-RFP, which, when expressed alone in N2a cells, colocalized with phalloidin-stained F-actin. When GFP-Lfc and neurabin-RFP were coexpressed, both proteins were again found to coaccumulate, often highly concentrated in single puncta at the cell periphery. These punctate regions also stained heavily for F-actin (Figures 8E–8H) but did not contain any enrichment for tubulin (Figures 8I–8L).

In contrast to full-length Lfc, coexpression of neurabin-RFP with Lfc(1–700) (lacking the coiled-coil domain) did not lead to coaccumulation of the two proteins (Figures 8M–8O). Similarly, coexpression of full-length Lfc with neurabin(Δ285)-RFP (lacking the F-actin binding domain) did not lead to coaccumulation (Figures 8P–8R). Mutation of Phe460 of neurabin to Ala (a mutation that would prevent binding of PP1 [Hsieh-Wilson et al., 1999]) had no influence on coaccumulation of neurabin and Lfc (data not shown). Coexpression of the Rho C3 inhibitor protein with GFP-Lfc and neurabin-RFP prevented their punctate coaccumulation, and Lfc and neurabin largely displayed nonoverlapping distributions (Figures 8S–8U). Moreover, coaccumulation was not observed when neurabin-RFP was coexpressed with GFP-Lfc(ΔDH), a mutant lacking the GEF enzymatic domain (data not shown). Importantly, in the absence of any association between neurabin and Lfc, or in the presence of the C3 inhibitor, F-actin accumulation did not occur (as demonstrated using staining with phalloidin; data not shown). Similar results were obtained when full-length Myc-spinophilin was coexpressed with GFP-Lfc; the proteins clustered together with F-actin, and this was prevented by coexpression with C3 inhibitor (data not shown).

### Lfc Regulates Spine Morphology

Together, these data indicate that either neurabin or spinophilin can organize the relocalization of Lfc from

14DIV (K) or 17DIV (L). (K) The translocation of GFP-Lfc caused by treatment with 90 mM $K^+$ was significantly attenuated by $Ni^{2+}$ (n = 200 spine/shaft pairs, four cells, and two independent experiments). (Inset) Fura2 $Ca^{2+}$ imaging in dentate gyrus neurons showed that $Ni^{2+}$ treatment resulted in a large decrease in $Ca^{2+}$ influx upon stimulation with 90 mM $K^+$. (L) GFP-Lfc-expressing neurons treated with a combination of 100 μM APV and 10 μM nimodipine showed no significant translocation upon stimulation with 50 Hz for 20 s (n = 179 spine/shaft pairs, two cells, and two independent experiments). APV and nimodipine were added ~5 min prior to stimulation and were present throughout the subsequent analysis. (Inset) Fura2 $Ca^{2+}$ imaging showed that the $Ca^{2+}$ influx induced by 50 Hz, 20 s field stimulation was reduced by pretreatment with APV plus nimodipine.

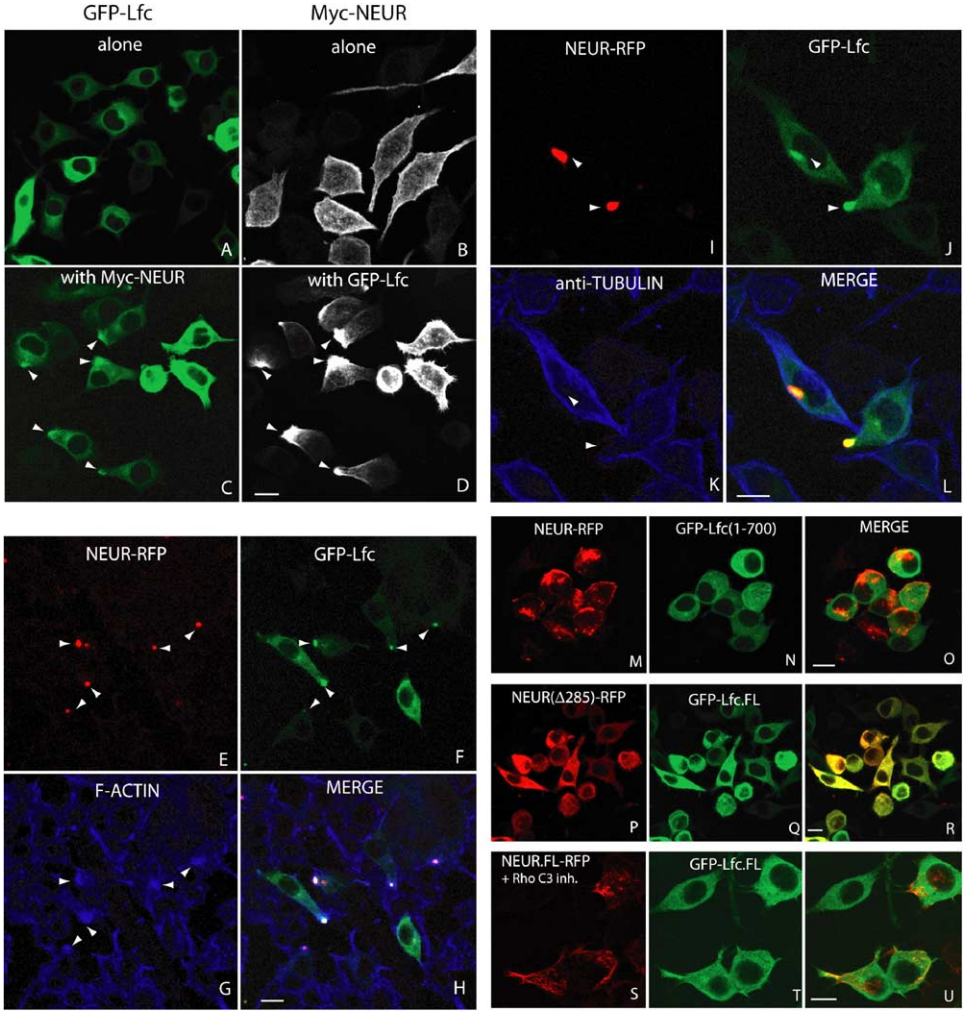


Figure 8. Interaction of Neurabin and Lfc Regulates the Actin Cytoskeleton in a Rho-Dependent Manner

(A–D) GFP-Lfc (green) and Myc-neurabin (white) were expressed either alone (A and B) or together (C and D) in N2a cells, and their distributions were studied by analysis of GFP fluorescence (GFP-Lfc) or by detection using an anti-Myc antibody (Myc-neurabin). Arrowheads point to regions in cells coexpressing both proteins where Lfc and neurabin coaccumulate. Coaccumulation was quantified in cells (with equivalent expression levels of GFP-Lfc and Myc-neurabin) by comparing the clustering of the two signals within a circular area of ~11 μM diameter. Clustering of both signals was observed in 81% ± 11% of cells (mean ± SD; >260 cells from three separate experiments). N2a cells expressing GFP-Lfc displayed a more rounded morphology with fewer neuritic protrusions compared to untransfected cells in the same culture, as might be expected following activation of the Rho signaling pathway.

(E–H) Neurabin-RFP (red) and GFP-Lfc (green) were coexpressed in N2a cells, and their distribution was compared to that of F-actin detected using phalloidin (blue). (H) shows a merge of the signals in (E)–(G). Arrowheads point to regions of cells where the density of F-actin, Lfc, and neurabin is high. Clustering of both RFP and GFP signals was observed in 95% ± 5% of cells (mean ± SD, 210 cells from three separate experiments).

(I–L) Neurabin-RFP (red) and GFP-Lfc (green) were coexpressed in N2a cells, and their distribution was compared to that of tubulin detected using a specific antibody (blue). (L) shows a merge of the signals in (I)–(K). Arrowheads point to regions of high density of Lfc and neurabin but not tubulin.

(M–O) Neurabin-RFP (red) and GFP-Lfc(1–700) (green) were coexpressed in N2a cells, and their distribution was compared. Clustering of both RFP and GFP signals was observed in 5% ± 5% of cells (mean ± SD, 155 cells from two separate experiments).

(P–R) Neurabin(286–1095)-RFP [Neur(Δ285)-RFP; red] and GFP-Lfc(1–700) (green) were coexpressed in N2a cells, and their distribution was compared. Clustering of both RFP and GFP signals was observed in 1% ± 1% of cells (mean ± SD, 210 cells from three separate experiments).

(S–U) Neurabin-RFP (red) and GFP-Lfc (green) were coexpressed in N2a cells together with the rho C3 inhibitor, and the distribution of neurabin and Lfc was compared. Clustering of both RFP and GFP signals was observed in 16% ± 10% of cells (mean ± SD, 90 cells from three separate experiments). (O), (R), and (U) show merged images. Scale bars, 10 μm.

microtubules to the F-actin cytoskeleton and that the clustering of Lfc, neurabin (or spinophilin), and F-actin occurs in a Rho-dependent manner. The interaction between neurabin or spinophilin and Lfc may therefore play an important role in the organization of the actin cytoskeleton in dendritic spines. We investigated this possibility by expressing Lfc in dentate gyrus neurons (Figure 9). Expression of full-length GFP-Lfc significantly decreased spine length and spine area (Figures 9A and 9D and Figures 9B and 9F; quantitation in Fig-

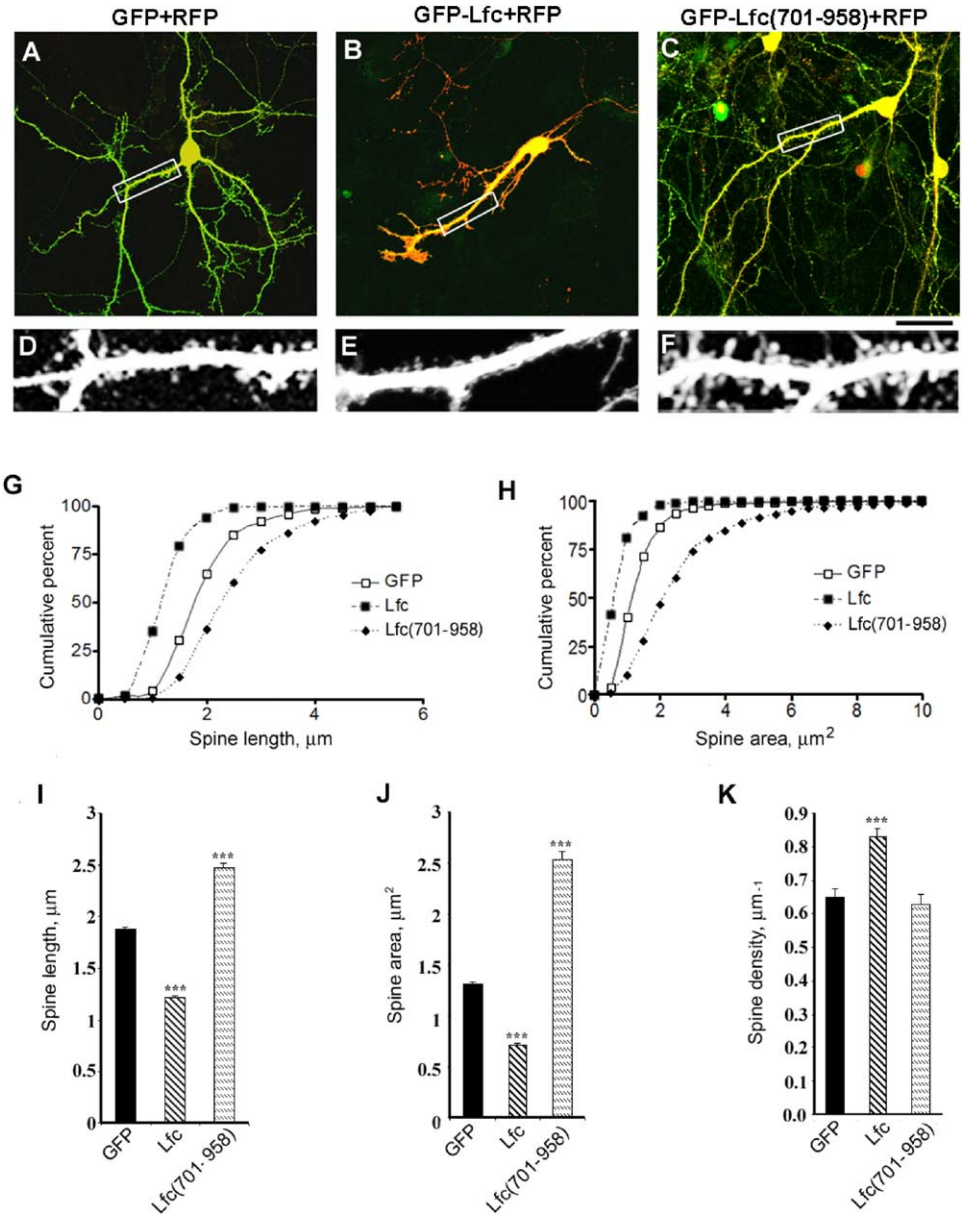


Figure 9. Full-Length Lfc and the Coiled-Coil Domain of Lfc Have Opposite Effects on Spine Morphology

Dentate gyrus neurons were transfected at 7DIV–8DIV and imaged at 17DIV–21DIV. RFP was used as a volume marker to monitor changes in cell morphology. (A) Control neurons show normal spine morphology with typical mushroom-shaped spines (n = 1439 spines from 15 cells and four independent experiments). (B) Neurons expressing GFP-Lfc have a simpler dendritic morphology and shorter and smaller spines (n = 898 spines from ten cells and four independent experiment). (C) Neurons expressing GFP-Lfc(701–958) show longer spines (n = 528 spines from six cells and three independent experiments). Scale bar, 60 μm. (D–F) Close views of the selected segments as shown in (A)–(C). Cumulative distributions of spine length (I) and spine area (H). Histograms of mean spine length (I), spine area (J), and spine density (K). Values are mean ± SEM; ***p < 0.001 (one-way ANOVA).

ures 9G–9J). Expression of GFP-Lfc also resulted in an increase in spine density (Figure 9K). Preliminary results indicate that the effect of Lfc on spine morphology depends on Rho and Rho kinase activity (J.A., X.P.R., P.G., A.C.N., G.-Y.W., unpublished data). We also investigated whether the coiled-coil domain of Lfc might act in a dominant-negative fashion. Expression of GFP-Lfc(701–958) had the opposite effect to that of the full-length protein, with a significant increase in spine length and spine area being measured (Figures 9C and 9F; quantitation in Figures 9G–9J). However, expression of GFP-Lfc(701–958) had no effect on spine density (Figure 9K).

Consistent with the hypothesis that neurabin/spinophilin serve to localize Lfc to F-actin in spines where it can activate Rho, we observed that expression of GFP-neurabin(1–485), a truncated protein that lacks the coiled-coil domain and would not interact with endoge-

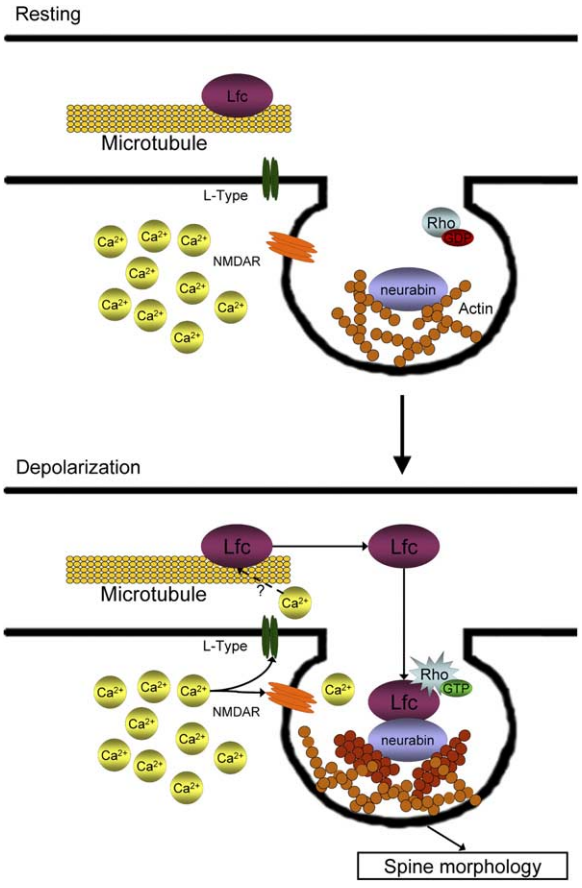


Figure 10. Model of Regulation of Rho in Dendritic Spines

Under resting conditions (upper panel), Lfc is located mainly in dendrites, where it is maintained in an inactive or sequestered state through interaction with microtubules. Neurabin (or spinophilin [data not shown]) is located mainly in dendritic spines through its association with F-actin. Rho is found mainly in its inactive, GDP bound state. Following membrane depolarization through activation of NMDA receptors and L-type $Ca^{2+}$ channels, Lfc is released from microtubules. By virtue of its specific interaction with neurabin or spinophilin, Lfc is targeted to dendritic spines, where it can activate Rho and cause alterations in spine morphology.

nous Lfc, also appeared to act in a dominant-negative fashion. Compared to control untransfected neurons, or cells expressing full-length GFP-neurabin, dendritic protrusions (filopodia or spines) in neurons expressing GFP-neurabin(1–485) were extraordinarily thin and long, being on average four times the normal length. As determined by the juxtaposition of GFP-neurabin(1–485) with the presynaptic marker synapsin, synapses appeared to form on the heads of the extended filopodia (Figure S4). Coexpression studies demonstrated that full-length neurabin exhibited a dominant effect over the action of neurabin(1–485), supporting the idea that neurabin(1–485) acts in a dominant-negative manner (Figure S4 and data not shown). Similar results were obtained following expression of truncated spinophilin proteins lacking the coiled-coil domain (S. Grossman and P.G., unpublished data). Recent studies by Svoboda and colleagues have also found that overexpression of the actin binding domain of neurabin increases spine length (Zito et al., 2004). Our current results support the conclusion that GFP-neurabin(1–485) (or comparable spinophilin fragments) can act as dominant-negative molecules that displace endogenous neurabin/spinophilin and occlude potential regulation of Rho and the F-actin cytoskeleton by Lfc.

## Discussion

In the present study, we have demonstrated and characterized the interaction of the Rho GEF Lfc with neurabin and spinophilin. Neurabin and spinophilin are preferentially expressed in neurons, where they are highly localized to dendritic spines via an interaction with F-actin. While a role for the Rho family of small GTPases (including RhoA, -B, -C, and -G isoforms; Rac; and cdc42) has been implicated in various aspects of axonal and dendritic development and maintenance (Luo, 2000), fewer studies have directly addressed the role of these GTPases in dendritic spines (Govek et al., 2004; Nakayama et al., 2000; Penzes et al., 2003; Scott et al., 2003; Tashiro et al., 2000). Moreover, little is known about the mechanisms involved in the regulation of the Rho family GTPases, particularly Rho, in dendrites and spines. The results obtained in the present study suggest a mechanism by which neurabin or spinophilin contributes to the organization of the F-actin cytoskeleton in dendritic spines, and in turn to the regulation of spine morphology, via the activity-dependent recruitment of the Rho-specific GEF Lfc (see model in Figure 10). Under resting conditions, neurabin and spinophilin are localized primarily within dendritic spines through their interaction with F-actin, while Lfc is primarily localized in the dendritic shaft through its interaction with microtubules. Upon neuronal stimulation, Lfc is released from its interaction with microtubules, whereupon it accumulates in spines through interaction with neurabin/spinophilin. The neurabin/spinophilin/Lfc complex then would locally activate Rho through the GEF activity of Lfc, leading to the stabilization of F-actin cytoskeleton in spines, and a reduction in spine size (not illustrated in Figure 10).

A truncated form of Lfc was first identified as part of an expression cloning study to find novel oncogenes and was named based on its relationship to Lbc, a previously cloned Cdc24-like GEF (Glaven et al., 1996; Whitehead et al., 1995). The truncated Lfc was distinct from Lbc in that, in addition to the DH and PH domains, it also contained an N-terminal cysteine- and histidine-rich domain (C1) similar to that found in the diacylglycerol binding domain of PKC and other proteins. Expression of truncated Lfc resulted in transformation of NIH 3T3 cells, a result that required the DH and PH domains but did not require the C1 domain. The full-length DNA for human Lfc (termed GEF-H1) was identified in another screen for genes that cause proliferation (Ren et al., 1998). These earlier studies, together with more recent studies of the truncated (Glaven et al., 1999) or full-length (Krendel et al., 2002) protein, concluded that Lfc exhibited specificity for Rho. There is some evidence that Lfc can bind to and perhaps activate Rac in vitro (Glaven et al., 1996; Ren et al., 1998), and over-

expression of Lfc in COS cells was found to activate Jun kinase in a Rac-dependent manner (Glaven et al., 1999). However, in our biochemical studies in neurons, full-length Lfc exhibited specificity for Rho. Moreover, the ability of coexpression of Lfc and neurabin to organize the F-actin cytoskeleton was dependent on Rho activity.

The Rho GTPases play a variety of roles during neuronal development as well as in mature neurons. The prevailing view is that Rac and cdc42 generally promote, while Rho (most studies are limited to RhoA) limits, growth of axons and dendrites (Luo, 2000; Shamah et al., 2001; Sin et al., 2002). While less is known about the role of Rho family GTPases in spine morphogenesis, it also appears that Rac and Rho have opposing roles (Nakayama et al., 2000; Tashiro et al., 2000). Activation of Rac1 promotes the formation of spines (Bryan et al., 2004; Nakayama et al., 2000; Penzes et al., 2003; Tolias et al., 2005). In contrast, brief expression of active RhoA in mature neurons in cortical or hippocampal slices results in stabilization of shorter spines (Tashiro et al., 2000). Moreover, inhibition of Rho or Rho kinase results in a dramatic increase in the length of spine necks (Tashiro et al., 2000; Tashiro and Yuste, 2004). This latter phenotype is very similar to what we observed following expression in neurons of GFP-neurabin(1–485) presumably acting as a dominant-negative F-actin binding protein to displace neurabin/spinophilin. A somewhat similar phenotype of longer spines was observed in immature neurons isolated from spinophilin-deficient mice (Feng et al., 2000). Thus, inhibition of Rho and disregulation of the spinophilin/neurabin/Lfc complex have similar effects on spine morphology that are likely to be caused by perturbation of the local influence of this protein complex on the F-actin cytoskeleton in spines.

The actin cytoskeleton is believed to be critical both for the initial formation of synaptic spines, as well as for the maintenance and plasticity of spines at mature synapses (Halpain, 2000; Matus, 2000; Segal and Andersen, 2000; Yuste and Bonhoeffer, 2004). Several Rho family GEFs, including kalirin (Penzes et al., 2003), GEFT (Bryan et al., 2004), Tiam-1 (Tolias et al., 2005), and PIX (Zhang et al., 2005), have been implicated in spine morphogenesis. A common feature of these GEFs is that they appear specific for activation of Rac1 and that they likely contribute to the formation of spines and to initial aspects of synapse formation. In contrast, Lfc, through the specific activation of Rho, is likely involved in the regulation of the actin cytoskeleton in mature synapses. Glutamate acting at NMDA and AMPA receptors has been associated with stabilization or maturation of spines, a process that appears to involve inhibition of actin dynamics and formation of more stable actin filaments in the center of spines (Fischer et al., 2000; Star et al., 2002). Long-term potentiation is associated with NMDA-dependent increases in spine number or spine size (Engert and Bonhoeffer, 1999; Maletic-Savatic et al., 1999; Matsuzaki et al., 2004; Ostroff et al., 2002). However, recent studies have demonstrated bidirectional regulation of spine morphology, with protocols associated with long-term depression leading to shrinkage or retraction of spines (Nagerl et al., 2004; Okamoto et al., 2004; Zhou et al., 2004). The translocation of Lfc from the dendritic shaft into dendritic spines, and the local activation of Rho via neurabin/spinophilin/Lfc, may represent one of the molecular mechanisms whereby glutamate can stabilize F-actin within spines and contribute to the bidirectional regulation of spine morphology.

While it is clear that the F-actin cytoskeleton plays a critical role in the formation, motility, and stabilization of dendritic spines, there are likely to be contributions from numerous proteins that are involved in various aspects of F-actin organization. Like Lfc, the actin binding proteins profilin (Ackermann and Matus, 2003) and cortactin (Hering and Sheng, 2003) move into and out of spines, respectively, in an activity-dependent fashion. β-catenin, a protein involved in interactions between adhesion molecules and the actin cytoskeleton, also redistributes into spines in response to depolarization (Murase et al., 2002). Given that numerous signal transduction molecules and their scaffolding proteins function in a coordinated fashion in dendritic spines, it is not surprising that several important regulatory proteins exhibit activity-dependent translocation into and out of spines. In the case of Lfc, profilin, and cortactin, their redistribution would likely be associated with stabilization of F-actin in spines.

Our results indicate a role for activation of NMDA receptors by glutamate, and consequently $Ca^{2+}$ influx via NMDA receptors and L-type $Ca^{2+}$ channels, in the redistribution of Lfc to spines. The release of Lfc from microtubules may involve phosphorylation of Lfc or a putative Lfc or microtubule binding protein. Preliminary results indicate that Lfc is phosphorylated at multiple sites (data not shown), and stimulation of NMDA-dependent signaling pathways may lead to either $Ca^{2+}$-dependent phosphorylation or dephosphorylation of Lfc. Previous studies by Krendel and coworkers have raised the possibility that Lfc (GEF-H1) is inactive when bound to microtubules in HeLa cells (Krendel et al., 2002). However, whether Lfc is present in an inactive state while bound to microtubules or is just sequestered from Rho is not clear. Our preliminary studies indicate that the coiled-coil domain of Lfc is not involved in its interaction with microtubules, but that the C1 domain is required for this association. The C1 domain does not resemble known microtubule binding motifs. In addition, our studies have indicated that purified bacterial full-length Lfc did not coprecipitate with microtubules (data not shown), a result consistent with preliminary studies carried out by Krendel and coworkers. Thus, binding of Lfc to microtubules may be indirect.

The results from this and other studies also highlight the growing appreciation that interactions occur between the microtubule and actin cytoskeletons (Fuchs and Karakesisoglou, 2001; Rodriguez et al., 2003; Salmon et al., 2002; Wittmann and Waterman-Storer, 2001). In neurons, a dynamic interplay exists between microtubules and actin in axonal growth cones, and local regulation of the actin cytoskeleton by Rho plays an important role in axon guidance and branching (Buck and Zheng, 2002; Liu and Strittmatter, 2001; Rodriguez et al., 2003; Schaefer et al., 2002). In addition to Lfc, several other Rho family GEFs, such as p190Rho GEF (van Horck et al., 2001), trioGEF1 (Bellanger et al., 1998; Blangy et al., 2000), Asef (Kawasaki et al., 2000), and

Tiam-1 (Kunda et al., 2001), appear to colocalize with microtubules, supporting the idea that GEFs mediate the coordination between the microtubule and actin filaments. Our present results highlight the role of microtubule binding of Lfc in dendrites, and in the selective regulation of the actin cytoskeleton in dendritic spines.

## Experimental Procedures

See the Supplemental Data for additional description of Experimental Procedures.

### Hippocampal Primary Culture and Transfection

Hippocampi were dissected from embryonic day (E) 18–19 rat embryos, dissociated, and plated at a density of $\sim 0.8 \times 10^5/cm^2$ on poly-lysine-coated glass coverslips (BD Labware) as described (Goslin et al., 1998). Neuronal cultures were grown in Neurobasal medium (Gibco BRL) supplemented with B27 (Gibco BRL) and 0.5 mM glutamine.

Neurons (3DIV–10DIV) were transfected using calcium phosphate (Craig, 1998). Before transfection, the conditioned culture media were removed and saved. Neurons were incubated with 1 ml of fresh Neurobasal medium (per well of a 12-well plate) containing 25 mM HEPES (pH 7.3). During this time, the DNA/calcium phosphate precipitate was prepared by mixing one volume of 10 μg of DNA in 250 mM $CaCl_2$ with an equal volume of 2× HBS ("CalPhos" mammalian transfection kit; Clontech). The precipitate was allowed to form for 2 min at room temperature before addition to the culture. DNA/calcium phosphate suspension (100 μl) was added drop-wise to each 22 mm diameter well (a total of 6 wells per transfection). After a 15 min incubation, when a layer of precipitate became obvious, cells were washed three times with Neurobasal medium and returned to the saved growth medium.

N2a cells were transfected using FuGENE 6 (Roche) at the ratio of 2–4 μg DNA:12 μl FuGENE6 in a 6 cm culture dish (Corning).

### DiI or Phalloidin Staining, Immunocytochemistry, and Confocal Microscopy

Lipophilic tracer DiI (1,1′-dioctadecyl-3,3,3′,3′-tetramethyl-indocarbocyanine perchlorate; Molecular Probes) was used to stain neurons. Neurons were fixed for 20 min in PBS with 4% paraformaldehyde, washed with PBS, and incubated in PBS containing 2.5 μg/ml DiI (diluted from a stock solution of 5 mg/ml in DMSO) for 1 min. The DiI solution was then removed, and samples were incubated in PBS at room temperature for 1 hr for dye to permeate. Samples were examined using a rhodamine filter.

Alexa Fluor 568 phalloidin and BODIFY 650/665 phalloidin (Molecular Probes) were used to stain F-actin filaments. Fixed and permeabilized cells (as described in immunocytochemistry below) were incubated in PBS containing fluorescent phalloidin (5 units/ml, diluted from a 200 units/ml stock solution in methanol) for 20 min at room temperature, washed three times with PBS, and mounted.

For immunocytochemistry, cells were fixed for 20 min at room temperature with 4% paraformaldehyde in PBS. They were permeabilized with 0.3% Nonidet P-40 for 5 min, washed, and preincubated with 10% donkey serum (Jackson ImmunoResearch) in PBS. Primary antibodies (in PBS) were incubated with samples for 2 hr. Samples were then washed and incubated with secondary donkey anti-mouse, anti-rabbit, or anti-guinea pig antibodies (Jackson ImmunoResearch) for 1 hr. Samples were mounted and examined using a Zeiss LSM 510 confocal microscope. Images were taken using a 63×/1.2W objective. Multiple tracking mode was used for colocalization studies to minimize signal spillover.

In studies of colocalization of neurabin and actin in N2a cells (Figure S1) and neurons (Figure S4), colocalization of GFP and phalloidin signals was generated using the LSM510 confocal software (version 3.2). The subtraction ratio of the two signals was generated to facilitate quantification. Images of colocalization were generated from two separate signals, from which regions of cortical or filopodial areas were defined by the overlaid ovals (8 μm × 5 μm, three cortical or filopodial areas in each cell). The coefficients of colocalization measured by the Zeiss analysis tool for these selected regions were then recorded.

To quantitate the redistribution of Lfc and neurabin or spinophilin (Figure 8 and Figure S1), the LSM510 confocal software was also used to set a threshold value to one of the confocal channels. The same threshold was then automatically applied to the other confocal signal with the absolute signals being normalized by the Zeiss analysis software. Colocalized "puncta" from the RFP and GFP signals (within a circular area of 11 ± 4 μm) were measured. Colocalized puncta were scored positive, and the percentage of positive cells was calculated (the majority of cells contained one colocalized puncta).

### Analysis of the Effect of Lfc on Dendritic Structure

From images of transfected hippocampal neurons, the number of dendritic segments was counted as the sum of the numbers of dendritic branch points and dendrite terminal ends (Nakayama et al., 2000). For analysis of spine length (bar graph in Figure S4), images were superimposed with a line of 4 μm using Zeiss LSM 510 software, and the length of individual spines was determined to be either longer or shorter than 4 μm. Every spine on a randomly selected dendrite was measured in this way, and at least 200 spines were counted for each set of transfected neurons.

### Analysis of Translocation of Lfc and Role in Spine Morphology

Cultures of dentate gyrus-CA3 explants were obtained from P0–P2 rats, and calcium phosphate transfections were carried out at 5DIV–8DIV as previously described (Wu et al., 2001). Prior to stimulation, cultured neurons were preincubated in 1 μM TTX Tyrode's solution for ~1 hr to block spontaneous neuronal activity; TTX was also present during the poststimulus phase. Individual transfected neurons were maintained in a continuous perfusion chamber at room temperature and visualized with a 40× oil immersion objective (NA 1.0) using a Zeiss LSM 510 META laser scanning microscope. Cells were stimulated by rapidly perfusing 90 mM KCl in isotonic Tyrode's solution for 3 min.

Field electrical stimulation was conducted via a pair of platinum electrodes connected to a high constant current isolator (WPI, 30 mA, 1 ms in duration). To block spontaneous $Ca^{2+}$ oscillation, most of the field stimulation experiments were done with 1 mM $Ca^{2+}$/4 mM $Mg^{2+}$ Tyrode's solution. In some of the experiments, $Ca^{2+}$ influx was blocked pharmacologically by the application of $Ni^{2+}$ (2 mM), or nimodipine (10 μM) plus APV (100 μM). A U-shaped fast perfusion tube controlled by an electrical valve was used for fast exchange of solution, and the inhibitors were added 5–10 min prior to stimulation. In some experiments, the $Ca^{2+}$ transients evoked by field electrical stimulation or high-$K^+$ depolarization were also monitored (Wu et al., 2001).

Standard confocal microscopy techniques using stacked Z-series data were employed to rule out artifacts from shifting focus or changes in dendrite positioning. Within the same experimental group, the imaging parameters were kept constant, with the brightest signal set to fit to the maximal dynamic range. A 50–100 μm primary dendrite from each imaged neuron was used, and each individual spine present on the dendrite was included. In most cases, cells were cotransfected with a red version of cytosolic fluorescent protein (DsRed; Clontech) to visualize detailed morphology and to outline the spines. Areas of interest were chosen based on the red channel. The mean of fluorescence intensity from the GFP-Lfc channel was measured in three adjacent areas—spine, shaft, and background—using ImageJ or Adobe Photoshop. Data were accumulated from multiple cells, and the ratio of corrected (subtracted background) spine intensity to corrected shaft intensity was determined and compared before and after stimulation.

### Supplemental Data

The Supplemental Data include Experimental Procedures and four figures and can be found with this article online at http://www.neuron.org/cgi/content/full/47/1/85/DC1/.

### Acknowledgments

We thank Panos Anastasiadis and Albert Reynolds for providing plasmids; Michael Rosen for helpful discussions; and Rowena Al-

monte-Baldonado for assistance with primary neuronal cultures. Supported by USPHS grants MH40899 and DA10044 (A.C.N., P.B.A., and P.G.) and DA17919 (G.-Y.W.), and by US Army grant W81XWH-04-1-0260 (G.-Y.W.).

Received: September 10, 2003
Revised: January 24, 2004
Accepted: May 6, 2005
Published: July 6, 2005

## References

Ackermann, M., and Matus, A. (2003). Activity-induced targeting of profilin and stabilization of dendritic spine morphology. Nat. Neurosci. *6*, 1194–1200.

Allen, P.B., Ouimet, C.C., and Greengard, P. (1997). Spinophilin, a novel protein phosphatase 1 binding protein localized to dendritic spines. Proc. Natl. Acad. Sci. USA *94*, 9956–9961.

Allen, P.B., Hsieh-Wilson, L., Yan, Z., Feng, J., Ouimet, C.C., and Greengard, P. (1999). Control of protein phosphatase I in the dendrite. Biochem. Soc. Trans. *27*, 543–546.

Bellanger, J.M., Lazaro, J.B., Diriong, S., Fernandez, A., Lamb, N., and Debant, A. (1998). The two guanine nucleotide exchange factor domains of Trio link the Rac1 and the RhoA pathways in vivo. Oncogene *16*, 147–152.

Benard, V., Bohl, B.P., and Bokoch, G.M. (1999). Characterization of rac and cdc42 activation in chemoattractant-stimulated human neutrophils using a novel assay for active GTPases. J. Biol. Chem. *274*, 13198–13204.

Blangy, A., Vignal, E., Schmidt, S., Debant, A., Gauthier-Rouviere, C., and Fort, P. (2000). TrioGEF1 controls Rac- and Cdc42-dependent cell structures through the direct activation of rhoG. J. Cell Sci. *113*, 729–739.

Blomberg, N., Baraldi, E., Nilges, M., and Saraste, M. (1999). The PH superfold: a structural scaffold for multiple functions. Trends Biochem. Sci. *24*, 441–445.

Bonhoeffer, T., and Yuste, R. (2002). Spine motility. Phenomenology, mechanisms, and function. Neuron *35*, 1019–1027.

Bryan, B., Kumar, V., Stafford, L.J., Cai, Y., Wu, G., and Liu, M. (2004). GEFT, a Rho family guanine nucleotide exchange factor, regulates neurite outgrowth and dendritic spine formation. J. Biol. Chem. *279*, 45824–45832.

Buchsbaum, R.J., Connolly, B.A., and Feig, L.A. (2003). Regulation of p70 S6 kinase by complex formation between the Rac guanine nucleotide exchange factor (Rac-GEF) Tiam1 and the scaffold spinophilin. J. Biol. Chem. *278*, 18833–18841.

Buck, K.B., and Zheng, J.Q. (2002). Growth cone turning induced by direct local modification of microtubule dynamics. J. Neurosci. *22*, 9358–9367.

Burnett, P.E., Blackshaw, S., Lai, M.M., Qureshi, I.A., Burnett, A.F., Sabatini, D.M., and Snyder, S.H. (1998). Neurabin is a synaptic protein linking p70 S6 kinase and the neuronal cytoskeleton. Proc. Natl. Acad. Sci. USA *95*, 8351–8356.

Craig, A.M. (1998). Transfecting cultured neurons. I. In Culturing Nerve Cells, G. Banker and K. Goslin, eds. (Cambridge, MA: MIT Press), pp. 79–112.

Engert, F., and Bonhoeffer, T. (1999). Dendritic spine changes associated with hippocampal long-term synaptic plasticity. Nature *399*, 66–70.

Etienne-Manneville, S., and Hall, A. (2002). Rho GTPases in cell biology. Nature *420*, 629–635.

Feng, J., Yan, Z., Ferreira, A., Tomizawa, K., Liauw, J.A., Zhuo, M., Allen, P.B., Ouimet, C.C., and Greengard, P. (2000). Spinophilin regulates the formation and function of dendritic spines. Proc. Natl. Acad. Sci. USA *97*, 9287–9292.

Fischer, M., Kaech, S., Knutti, D., and Matus, A. (1998). Rapid actin-based plasticity in dendritic spines. Neuron *20*, 847–854.

Fischer, M., Kaech, S., Wagner, U., Brinkhaus, H., and Matus, A. (2000). Glutamate receptors regulate actin-based plasticity in dendritic spines. Nat. Neurosci. *3*, 887–894.

Fuchs, E., and Karakesisoglou, I. (2001). Bridging cytoskeletal intersections. Genes Dev. *15*, 1–14.

Fukazawa, Y., Saitoh, Y., Ozawa, F., Ohta, Y., Mizuno, K., and Inokuchi, K. (2003). Hippocampal LTP is accompanied by enhanced F-actin content within the dendritic spine that is essential for late LTP maintenance in vivo. Neuron *38*, 447–460.

Glaven, J.A., Whitehead, I.P., Nomanbhoy, T., Kay, R., and Cerione, R.A. (1996). Lfc and Lsc oncoproteins represent two new guanine nucleotide exchange factors for the Rho GTP-binding protein. J. Biol. Chem. *271*, 27374–27381.

Glaven, J.A., Whitehead, I., Bagrodia, S., Kay, R., and Cerione, R.A. (1999). The Dbl-related protein, Lfc, localizes to microtubules and mediates the activation of Rac signaling pathways in cells. J. Biol. Chem. *274*, 2279–2285.

Goslin, K., Asmussen, H., and Banker, G. (1998). Rat hippocampal neurons in low-density culture. In Culturing Nerve cells, G. Banker and K. Goslin, eds. (Cambridge, MA: MIT Press), pp. 339–370.

Govek, E.E., Newey, S.E., Akerman, C.J., Cross, J.R., Van der Veken, L., and Van Aelst, L. (2004). The X-linked mental retardation protein oligophrenin-1 is required for dendritic spine morphogenesis. Nat. Neurosci. *7*, 364–372.

Grossman, S.D., Hsieh-Wilson, L.C., Allen, P.B., Nairn, A.C., and Greengard, P. (2002). The actin-binding domain of spinophilin is necessary and sufficient for targeting to dendritic spines. Neuromolecular Med. *2*, 61–69.

Halpain, S. (2000). Actin and the agile spine: how and why do dendritic spines dance? Trends Neurosci. *23*, 141–146.

Hering, H., and Sheng, M. (2003). Activity-dependent redistribution and essential role of cortactin in dendritic spine morphogenesis. J. Neurosci. *23*, 11759–11769.

Hsieh-Wilson, L.C., Allen, P.B., Watanabe, T., Nairn, A.C., and Greengard, P. (1999). Characterization of the neuronal targeting protein spinophilin and its interactions with protein phosphatase-1. Biochemistry *38*, 4365–4373.

Hsieh-Wilson, L.C., Benfenati, F., Snyder, G.L., Allen, P.B., Nairn, A.C., and Greengard, P. (2003). Phosphorylation of spinophilin modulates its interaction with actin filaments. J. Biol. Chem. *278*, 1186–1194.

Kawasaki, Y., Senda, T., Ishidate, T., Koyama, R., Morishita, T., Iwayama, Y., Higuchi, O., and Akiyama, T. (2000). Asef, a link between the tumor suppressor APC and G-protein signaling. Science *289*, 1194–1197.

Krendel, M., Zenke, F.T., and Bokoch, G.M. (2002). Nucleotide exchange factor GEF-H1 mediates cross-talk between microtubules and the actin cytoskeleton. Nat. Cell Biol. *4*, 294–301.

Kunda, P., Paglini, G., Quiroga, S., Kosik, K., and Caceres, A. (2001). Evidence for the involvement of Tiam1 in axon formation. J. Neurosci. *21*, 2361–2372.

Lisman, J.E., and Zhabotinsky, A.M. (2001). A model of synaptic memory: a CaMKII/PP1 switch that potentiates transmission by organizing an AMPA receptor anchoring assembly. Neuron *31*, 191–201.

Liu, B.P., and Strittmatter, S.M. (2001). Semaphorin-mediated axonal guidance via Rho-related G proteins. Curr. Opin. Cell Biol. *13*, 619–626.

Luo, L. (2000). Rho GTPases in neuronal morphogenesis. Nat. Rev. Neurosci. *1*, 173–180.

MacMillan, L.B., Bass, M.A., Cheng, N., Howard, E.F., Tamura, M., Strack, S., Wadzinski, B.E., and Colbran, R.J. (1999). Brain actin-associated protein phosphatase 1 holoenzymes containing spinophilin, neurabin, and selected catalytic subunit isoforms. J. Biol. Chem. *274*, 35845–35854.

Maletic-Savatic, M., Malinow, R., and Svoboda, K. (1999). Rapid dendritic morphogenesis in CA1 hippocampal dendrites induced by synaptic activity. Science *283*, 1923–1927.

Matsuzaki, M., Honkura, N., Ellis-Davies, G.C., and Kasai, H. (2004).

Structural basis of long-term potentiation in single dendritic spines. Nature *429*, 761–766.

Matus, A. (2000). Actin-based plasticity in dendritic spines. Science *290*, 754–758.

Murase, S., Mosser, E., and Schuman, E.M. (2002). Depolarization drives β-catenin into neuronal spines promoting changes in synaptic structure and function. Neuron *35*, 91–105.

Nagerl, U.V., Eberhorn, N., Cambridge, S.B., and Bonhoeffer, T. (2004). Bidirectional activity-dependent morphological plasticity in hippocampal neurons. Neuron *44*, 759–767.

Nakanishi, H., Obaishi, H., Satoh, A., Wada, M., Mandai, K., Satoh, K., Nishioka, H., Matsuura, Y., Mizoguchi, A., and Takai, Y. (1997). Neurabin: a novel neural tissue-specific actin filament-binding protein involved in neurite formation. J. Cell Biol. *139*, 951–961.

Nakayama, A.Y., Harms, M.B., and Luo, L. (2000). Small GTPases Rac and Rho in the maintenance of dendritic spines and branches in hippocampal pyramidal neurons. J. Neurosci. *20*, 5329–5338.

Nishizuka, Y. (1992). Intracellular signaling by hydrolysis of phospholipids and activation of protein kinase C. Science *258*, 607–614.

Okamoto, K., Nagai, T., Miyawaki, A., and Hayashi, Y. (2004). Rapid and persistent modulation of actin dynamics regulates postsynaptic reorganization underlying bidirectional plasticity. Nat. Neurosci. *7*, 1104–1112.

Oliver, C.J., Terry-Lorenzo, R.T., Elliott, E., Bloomer, W.A., Li, S., Brautigan, D.L., Colbran, R.J., and Shenolikar, S. (2002). Targeting protein phosphatase 1 (PP1) to the actin cytoskeleton: the neurabin I/PP1 complex regulates cell morphology. Mol. Cell. Biol. *22*, 4690–4701.

Ostroff, L.E., Fiala, J.C., Allwardt, B., and Harris, K.M. (2002). Polyribosomes redistribute from dendritic shafts into spines with enlarged synapses during LTP in developing rat hippocampal slices. Neuron *35*, 535–545.

Ouimet, C.C., da Cruz e Silva, E.F., and Greengard, P. (1995). The α and γ1 isoforms of protein phosphatase 1 are highly and specifically concentrated in dendritic spines. Proc. Natl. Acad. Sci. USA *92*, 3396–3400.

Penzes, P., Johnson, R.C., Sattler, R., Zhang, X., Huganir, R.L., Kambampati, V., Mains, R.E., and Eipper, B.A. (2001). The neuronal Rho-GEF Kalirin-7 interacts with PDZ domain-containing proteins and regulates dendritic morphogenesis. Neuron *29*, 229–242.

Penzes, P., Beeser, A., Chernoff, J., Schiller, M.R., Eipper, B.A., Mains, R.E., and Huganir, R.L. (2003). Rapid induction of dendritic spine morphogenesis by trans-synaptic ephrinB-EphB receptor activation of the Rho-GEF kalirin. Neuron *37*, 263–274.

Ren, Y., Li, R., Zheng, Y., and Busch, H. (1998). Cloning and characterization of GEF-H1, a microtubule-associated guanine nucleotide exchange factor for Rac and Rho GTPases. J. Biol. Chem. *273*, 34954–34960.

Ren, X.D., Kiosses, W.B., and Schwartz, M.A. (1999). Regulation of the small GTP-binding protein Rho by cell adhesion and the cytoskeleton. EMBO J. *18*, 578–585.

Rodriguez, O.C., Schaefer, A.W., Mandato, C.A., Forscher, P., Bement, W.M., and Waterman-Storer, C.M. (2003). Conserved microtubule-actin interactions in cell movement and morphogenesis. Nat. Cell Biol. *5*, 599–609.

Salmon, W.C., Adams, M.C., and Waterman-Storer, C.M. (2002). Dual-wavelength fluorescent speckle microscopy reveals coupling of microtubule and actin movements in migrating cells. J. Cell Biol. *158*, 31–37.

Satoh, A., Nakanishi, H., Obaishi, H., Wada, M., Takahashi, K., Satoh, K., Hirao, K., Nishioka, H., Hata, Y., Mizoguchi, A., and Takai, Y. (1998). Neurabin-II/spinophilin. An actin filament-binding protein with one pdz domain localized at cadherin-based cell-cell adhesion sites. J. Biol. Chem. *273*, 3470–3475.

Schaefer, A.W., Kabir, N., and Forscher, P. (2002). Filopodia and actin arcs guide the assembly and transport of two populations of microtubules with unique dynamic parameters in neuronal growth cones. J. Cell Biol. *158*, 139–152.

Scott, E.K., Reuter, J.E., and Luo, L. (2003). Small GTPase Cdc42 is required for multiple aspects of dendritic morphogenesis. J. Neurosci. *23*, 3118–3123.

Segal, M., and Andersen, P. (2000). Dendritic spines shaped by synaptic activity. Curr. Opin. Neurobiol. *10*, 582–586.

Shamah, S.M., Lin, M.Z., Goldberg, J.L., Estrach, S., Sahin, M., Hu, L., Bazalakova, M., Neve, R.L., Corfas, G., Debant, A., and Greenberg, M.E. (2001). EphA receptors regulate growth cone dynamics through the novel guanine nucleotide exchange factor ephexin. Cell *105*, 233–244.

Sin, W.C., Haas, K., Ruthazer, E.S., and Cline, H.T. (2002). Dendrite growth increased by visual activity requires NMDA receptor and Rho GTPases. Nature *419*, 475–480.

Star, E.N., Kwiatkowski, D.J., and Murthy, V.N. (2002). Rapid turnover of actin in dendritic spines and its regulation by activity. Nat. Neurosci. *5*, 239–246.

Stephens, D.J., and Banting, G. (2000). In vivo dynamics of the F-actin-binding protein neurabin-II. Biochem. J. *345*, 185–194.

Tashiro, A., and Yuste, R. (2004). Regulation of dendritic spine motility and stability by Rac1 and Rho kinase: evidence for two forms of spine motility. Mol. Cell. Neurosci. *26*, 429–440.

Tashiro, A., Minden, A., and Yuste, R. (2000). Regulation of dendritic spine morphology by the rho family of small GTPases: antagonistic roles of Rac and Rho. Cereb. Cortex *10*, 927–938.

Terry-Lorenzo, R.T., Carmody, L.C., Voltz, J.W., Connor, J.H., Li, S., Smith, F.D., Milgram, S.L., Colbran, R.J., and Shenolikar, S. (2002). The neuronal actin-binding proteins, neurabin I and neurabin II, recruit specific isoforms of protein phosphatase-1 catalytic subunits. J. Biol. Chem. *277*, 27716–27724.

Tolias, K.F., Bikoff, J.B., Burette, A., Paradis, S., Harrar, D., Tavazoie, S., Weinberg, R.J., and Greenberg, M.E. (2005). The Rac1-GEF Tiam1 couples the NMDA receptor to the activity-dependent development of dendritic arbors and spines. Neuron *45*, 525–538.

van Horck, F.P., Ahmadian, M.R., Haeusler, L.C., Moolenaar, W.H., and Kranenburg, O. (2001). Characterization of p190RhoGEF, a RhoA-specific guanine nucleotide exchange factor that interacts with microtubules. J. Biol. Chem. *276*, 4948–4956.

Wang, L.Y., Orser, B.A., Brautigan, D.L., and MacDonald, J.F. (1994). Regulation of NMDA receptors in cultured hippocampal neurons by protein phosphatases 1 and 2A. Nature *369*, 230–232.

Westphal, R.S., Tavalin, S.J., Lin, J.W., Alto, N.M., Fraser, I.D., Langeberg, L.K., Sheng, M., and Scott, J.D. (1999). Regulation of NMDA receptors by an associated phosphatase-kinase signaling complex. Science *285*, 93–96.

Whitehead, I., Kirk, H., Tognon, C., Trigo-Gonzalez, G., and Kay, R. (1995). Expression cloning of lfc, a novel oncogene with structural similarities to guanine nucleotide exchange factors and to the regulatory region of protein kinase C. J. Biol. Chem. *270*, 18388–18395.

Wittmann, T., and Waterman-Storer, C.M. (2001). Cell motility: can Rho GTPases and microtubules point the way? J. Cell Sci. *114*, 3795–3803.

Wu, G.Y., Deisseroth, K., and Tsien, R.W. (2001). Spaced stimuli stabilize MAPK pathway activation and its effects on dendritic morphology. Nat. Neurosci. *4*, 151–158.

Yan, Z., Hsieh-Wilson, L., Feng, J., Tomizawa, K., Allen, P.B., Fienberg, A.A., Nairn, A.C., and Greengard, P. (1999). Protein phosphatase 1 modulation of neostriatal AMPA channels: regulation by DARPP-32 and spinophilin. Nat. Neurosci. *2*, 13–17.

Yuste, R., and Bonhoeffer, T. (2004). Genesis of dendritic spines: insights from ultrastructural and imaging studies. Nat. Rev. Neurosci. *5*, 24–34.

Zhang, H., Webb, D.J., Asmussen, H., Niu, S., and Horwitz, A.F. (2005). A GIT1/PIX/Rac/PAK signaling module regulates spine morphogenesis and synapse formation through MLC. J. Neurosci. *25*, 3379–3388.

Zhou, Q., Homma, K.J., and Poo, M.M. (2004). Shrinkage of dendritic spines associated with long-term depression of hippocampal synapses. Neuron *44*, 749–757.

Zito, K., Knott, G., Shepherd, G.M., Shenolikar, S., and Svoboda, K. (2004). Induction of spine growth and synapse formation by regulation of the spine actin cytoskeleton. Neuron *44*, 321–334.